
UNIVERSITY OF NORTH TEXAS
HEALTH SCIENCE CENTER AT FORT WORTH
1970

Datta, Anjuli. Combined Chemo/Anti-Angiogenic Cancer Therapy in Lewis Lung Metastases. Master of Science (Microbiology and Immunology), May 2002. 41 pp., 17 illustrations, bibliography.

The focus of my dissertation studies is an eight amino acid peptide (Å6) derived from the non-receptor binding region of urokinase plasminogen activator (uPA), which partially inhibits the binding of uPA to its receptor (uPAR). Å6 has been synthesized as a potential novel anti-cancer agent and kindly provided by Ångstrom Pharmaceuticals, Inc. (San Diego, CA). We further examined potential therapeutic properties of Å6 *in vivo* and *in vitro*. Å6 appeared to directly inhibit the invasion of Lewis lung carcinoma cells through Matrigel by approximately 40-45% compared to control. In addition, Å6 had a morphological effect resulting in thicker tubes on small vessel endothelial tube formation compared to no treatment. Interestingly, doxorubicin had similar effects when added to growing endothelial cells. Moreover, Å6 was administered alone and in combination with a standard clinically used chemotherapeutic agent, doxorubicin, in a Lewis lung carcinoma mouse model to test possible synergy between an anti-angiogenic compound (Å6) and a chemotherapeutic agent. This is the first observation that Å6 has the potential to display a direct anti-metastatic therapeutic effect for established pulmonary metastases in this model. Therefore, we believe that Å6 in combination with doxorubicin has the potential to provide better therapy to cancer patients with tumor metastases than potent chemotherapeutic agents alone, by increasing the dose of non-toxic Å6 and reducing the recommended dose of doxorubicin.

COMBINED CHEMO/ANTI-ANGIOGENIC CANCER THERAPY IN LEWIS LUNG METASTASES

Anjuli Sinha-Datta, B.S., M.S.

APPROVED:

Ronald H Goldfarb
Major Professor

Committee Member

Committee Member

Hriday K. Das
University Member

Ronald H. Goldfarb
Chair, Department of Molecular Biology and Immunology

Graduate Dean

Combined Chemo/Anti-Angiogenic Cancer Therapy in Lewis Lung Metastases

THESIS

Presented to the Graduate Council of the

Graduate School of Biomedical Sciences

University of North Texas
Health Science Center at Fort Worth

in Partial Fulfillment of the Requirements

For the Degree of

MASTER OF SCIENCE

By

Anjuli Datta

Fort Worth, Texas

May 2002

ACKNOWLEDGEMENTS

First of all, I would like to thank my mentor, Dr. Ronald H. Goldfarb, for his guidance and continued support throughout my graduate career. In addition, a sincere "thanks" goes to Dr. Rick Kitson for his advice and willingness to answer all my questions. I would like to thank all my laboratory members: Yaming Xue, Gheath Al-Atrash, Wilson Chen, Ginelle Gellert, Kathleen Badeaux, Dr. Myoung Kim, and Min Lu, all whom have provided me with a friendly working environment and constant encouragement.

In addition, I would like to thank the professors who served on my committee, Dr. Neeraj Agarwal, Dr. Porunelloor Mathew, Dr. Hriday Das, Dr. Ronald H. Goldfarb, and my advisor, Dr. Jerry Simecka.

I would also like to thank Dr. Terence R. Jones and Dr. Andrew P. Mazar for supplying me with the anti-angiogenic compound Å6 (Ångstrom Pharmaceuticals, Inc. San Diego, CA).

Finally, I would like to thank my parents, Tapan and Rebecca Sinha, and brother Dev Sinha for their unconditional love and inspiration. I would like to thank my husband, Dr. Suman Datta, for his love and patience.

This research was funded by the Texas Advanced Technology Program # 000130-0080-1999.

TABLE OF CONTENTS

LIST OF TABLES AND ILLUSTRATIONS

Tables: Page

Figures:

CHAPTER 1

INTRODUCTION

Traditional modes of cancer therapy (i.e., radiation, chemotherapy, and surgery) have focused on the elimination of all transformed cells to attempt to obtain cures. However, approximately 50% of patients who develop malignant tumors fail to respond to these modalities and succumb to metastasis (1,2). Metastasis is defined as the "transfer of disease from one organ or part to another not directly connected with it (2). The process of metastasis can be described as a constant battle between the host's immune defense and the physical and biochemical properties of the invasive tumor cells. Similar to Darwin's theory of "survival of the fittest", the metastatic cascade is very selective. Only subpopulations within the primary tumor capable of surviving mechanical stress of blood flow and attack by host lymphoid effector cells (~1-2%) are capable of establishing secondary metastases. The existence of these heterogeneous subpopulations can have impact on elucidating tumor progression, invasiveness, and drug resistance (2,3). Invasive tumor cells must degrade components of the extracellular matrix (ECM), before extravasation into the lymph or blood circulation resulting in the formation of secondary tumors (4). As the sequence of events repeats itself, more aggressive and resistant tertiary, quaternary, etc...tumor sites are established.

In addition to metastasis, dose-limiting toxicities of several chemotherapeutic agents often compromise the patient's immune system, leading to morbidity and death. Early detection provides a better approach to treat metastatic cancer, but often the cancer has spread by the time it is visible to the naked eye. Unfortunately, highly invasive advanced metastatic tumors including carcinomas (i.e., breast, lung, prostate, and colon) are the most common tumor type found in humans. In many instances, standard chemotherapeutic treatments may actually increase the development of secondary tumor colonies by selecting for the most resistant and aggressive tumor cell populations (5). Therefore, there is an imperative need to find new approaches to treat established metastases. In order to understand the complex and dynamic process of metastasis, elucidation of mechanisms involved in tumor invasion and angiogenesis must be addressed.

Invasive tumor cells with metastatic potential produce several proteolytic enzymes that contribute to ECM destruction, in particular urokinase plasminogen activator (uPA) (1). Urokinase plasminogen activator is secreted as a single chain zymogen (411 amino acids). This serine protease consists of three domains: the growth factor domain (aa 1-48), kringle domain (aa 49-135), and the serine protease domain (aa 144-411). The growth factor domain is the determinant of uPA binding to its receptor (uPAR). The kringle domain is involved in protein-protein interaction, and the serine protease domain is responsible for the catalytic activity of uPA (6). Plasminogen activation is induced by the binding of uPA to its own high-affinity receptor (uPAR).

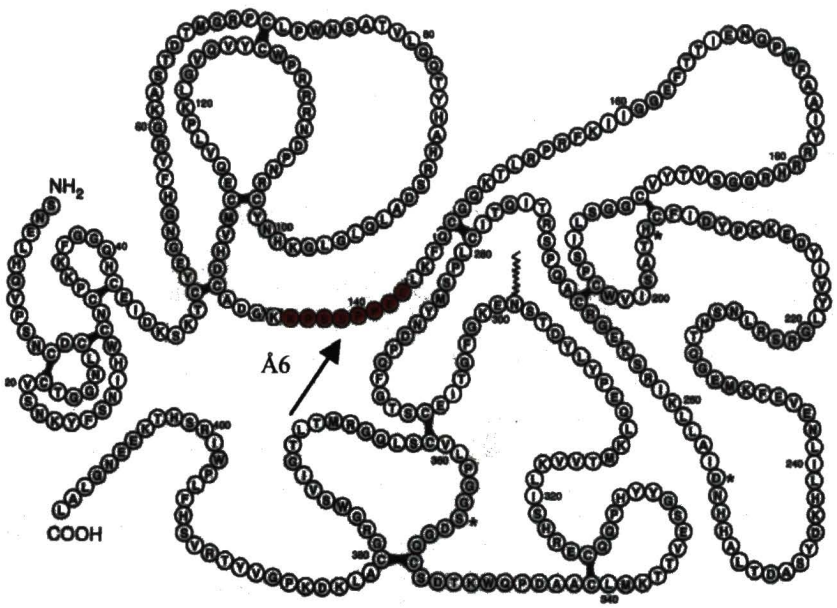

Urokinase Plasminogen Activator (uPA)

Primary sequence of uPA. Domains are defined as growth factor domain (aa 1-48), kringle domain (aa 49-135), Å6 (aa 136-143), and low MW uPA (aa 144-411).

Figure 1-uPA schematic modified by Andrew P. Mazar, Ph.D., Terence Jones, Ph.D., and Ronald H.Goldfarb, Ph.D.

Urokinase plasminogen activator receptor is a three-domain protein that is tethered to the external face of the plasma membrane via a glycosylphosphatidyl inositol (GPI) anchor. The receptor lacks both cytoplasmic and transmembrane domains, yet plays a role in signal transduction. This suggests association with transmembrane proteins (e.g. the integrin family) capable of linking ligand binding via uPAR to the cytoplasm (6,7). In the classical cascade of plasminogen activation, single-chain uPA (scuPA) binds to its surface receptor (uPAR) and is activated by plasmin to form two-chain uPA (tcuPA). Two-chain uPA is then able to cleave the zymogen form of plasmin (plasminogen) into active plasmin at the Arg561-Val562 bond (1,6). This autocrine cascade of plasminogen

activation results in the amplification of plasmin production that is capable of activating other downstream proteases (e.g. matrix metalloproteinases) (8), and directly degrading extracellular matrix components such as laminin and fibronectin (9). The plasminogen activation cascade is inhibited by plasminogen activator inhibitors (PAI) which bind uPA at a reactive center loop in the C-terminus (10). The uPA-PAI complex is degraded, while uPAR is recycled back to the cell surface.

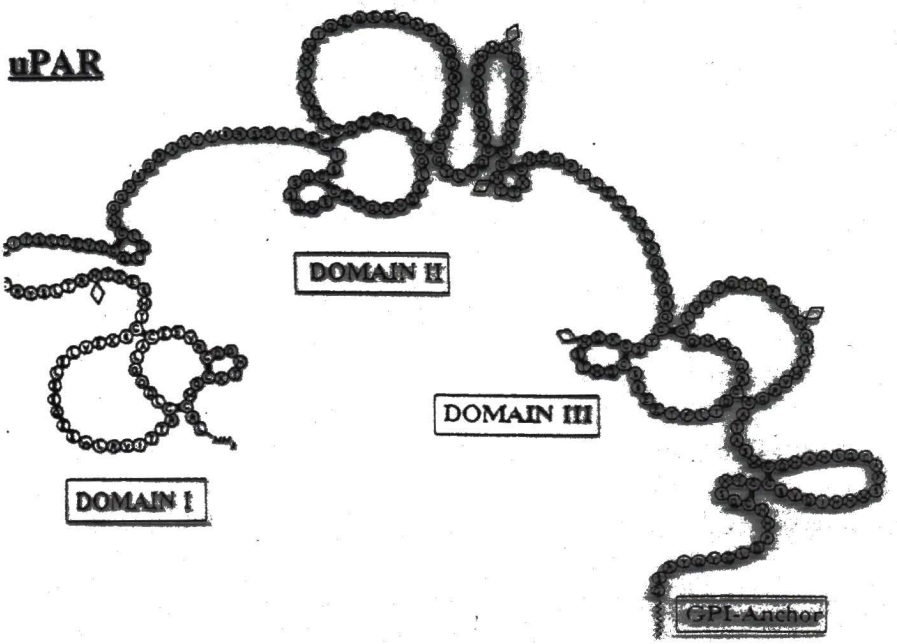

Figure 2-uPAR schematic modified by Andrew P. Mazar, Ph.D., Terence Jones, Ph.D., and Ronald H. Goldfarb, Ph.D.

Several studies correlate the expression of uPA and its receptor as a diagnostic tool for cancer prognosis. Although uPA and uPAR are expressed in non-cancerous cell types (i.e. natural killer cells (11), endothelial cells, and macrophages), several studies have indicated poor prognosis in metastatic cancers can be associated with the overexpression of uPA and/or uPAR (12,13). The uPA system is being targeted to treat cancer

metastases (i.e., uPAR antagonists, peptides based on the connecting region of uPA, and synthetic peptides which competitively inhibit the binding of uPA to uPAR) (5,6).

Moreover, our laboratory proposed a direct role for uPA in tumor angiogenesis and recent studies have extended this early work to implicate uPAR as well as uPA in the processes of neovascularization (1,14). Angiogenesis is defined as the growth of new blood vessels, involved in adult physiological processes like wound healing, the female reproductive cycle, and hair growth (15). Blood vessels are composed of endothelial cells, which form tubes that interconnect and maintain blood flow. Typically, endothelial cell turnover is very slow (measured in years), except under certain stimuli like cardiovascular disease, rheumatoid arthritis, or a tumor mass. Under these stresses, the quiescent nature of angiogenesis can be activated to grow new capillaries. First, endothelial cells emerge from venules lacking smooth muscle. Then basement membrane, a specialized ECM that invasive tumor cells must traverse, is degraded around the endothelial cell tube with the help of plasminogen activators and matrix metalloproteinases, the latter of which degrade type IV collagen (found only in basement membrane). This invasion is accompanied by the locomotion of endothelial cells toward the angiogenic stimulus (in this case a tumor) at the leading edge of what is now called a migrating column(16,17). The cells sprout and form a lumen. Then, the sprouts join each other to form capillary loops. Finally, a capillary network is formed from sprouts originating from capillary loops. This capillary network is able to then nourish the growing tumor from the host's circulation. Recently, a number of *in vitro* assays have

been established which are thought to mimic neovascularization and these have provided insight into possible mechanisms (18,19,20,21,22).

The dependency of tumor growth and progression on stimulators of neovascularization has peaked interest with "more than 300 endogenous, natural, or synthetic inhibitors of angiogenesis and 31 agents" presently in clinical trials (23). For instance, the nurturing of cancer cells from both primary tumors and distant metastases relies heavily on tumor vascularization. Failure of neovascularization results in tumor growth suppression and impaired metastasis (24). Therefore, without blood vessel formation, the tumor starves and its invasive and metastatic capabilities are severely inhibited. In addition, scientific evidence has noted that when a primary tumor is present, metastasis is suppressed by a circulating angiogenic inhibitor (termed angiostatin). Morever, partial removal of the primary tumor may increase the growth rate in the residual tumor (24, 25). The balance of angiogenic stimulators and inhibitors is complex, however crucial in understanding the mechanisms of tumor migration and invasion. Anti-angiogenic therapies in *in vivo* studies have shown significant reductions in tumor volume and metastases, and many are being evaluated in clinical trials (2,24,25,26, 27,28).

The focus of my dissertation studies is an eight amino acid peptide (Å6-aa 136-143) derived from the non-receptor binding region of uPA, that partially inhibits the binding of uPA to its receptor. Furthermore, Å6 inhibits the binding of single chain uPA to uPAR locking uPAR-dependent plasminogen activation (6, 29). Å6 has been shown to inhibit angiogenesis in glioblastoma and breast carcinoma *in vivo* (29, 30). Interestingly,

combination therapies using a potent chemotherapeutic agent in combination with an anti-angiogenic agent provide enhanced therapy compared to either agent alone (30, 31). Therefore, my proposal is globally directed towards developing novel approaches for cancer therapy using a standard chemotherapeutic agent (doxorubicin) and a novel anti-angiogenic compound (Å6).

I hypothesize that there will be synergistic or additive effects, by the use of an anti-angiogenic agent in combination with a standard anti-cancer chemotherapeutic agent. These effects include potential additivity of the combined agents against angiogenic blood vessel formation *in vitro*, and combination therapy *in vivo* using Å6 and doxorubicin compared to either agent alone. This hypothesis was investigated in a model of pulmonary Lewis Lung carcinoma metastases.

CHAPTER 2

METHODS

Cell culture:

Human fibrosarcoma (HT1080) and Lewis lung carcinoma (3LL) cells were maintained in 1640 RPMI medium supplemented with 10% fetal bovine serum (FBS), 1% Sodium Pyruvate, 1% Penicillin/Streptomycin, and 1% L-Glutamine. Adherent 3LL and HT1080 cells were detached from the flask using 0.2% EDTA solution.

Small vessel endothelial (SVEC) cells are SV40 transformed mouse endothelial cells. They were cultured in Dulbecco's modified minimal essential medium (DMEM) supplemented with 10% FBS, 1% Sodium Pyruvate, 1% Spreptomycin/Penicillin, and 1% L-Glutamine. Adherent SVEC monolayer was removed from the flask using a 0.25% trypsin solution. Cells were kept in a humidified incubator at 37°C with 5% CO_2.

Preparation of cell homogenates:

Confluent tumor cells were treated with a 0.2% EDTA solution to remove cells from the flask. Cells were then washed with RPMI twice, with a final resuspension of cells in 2 ml of RPMI. Cells were distributed into two Ependorf tubes containing one ml each of cell suspension. Next, the suspension was centrifuged at 700 rpm for 8 minutes. The supernatant was extracted and pellet discarded. Lysis of the cells was performed using a

freshly prepared kinase extraction buffer solution (10 mM Tris pH 7.4, 1% Triton X-100, 0.5% IGEPAL, 150 mM NaCl, 20 mM NaF, 1 mM EGTA, 1 mM EDTA, and ddH_20). Kinase extraction buffer (500 µl) was added to the cell supernatant. Cells were disrupted by vortex and ice in an alternating fashion for 15 minutes. The cell suspension was centrifuged at 700 rcf for 8 minutes and the supernatant was stored in -20°C.

Zymographic analysis:

This technique is used to demonstrate enzymatic activity (in this case urokinase plasminogen activator). In this experiment, enzymatic activity will yield a zone of lysis corresponding to the molecular weight of the enzyme. Absence of enzymatic activity will fail to display a zone of lysis. Enzymatic activity of uPA is observed by the conversion of plasminogen to plasmin, in which plasmin cleaves the protein casein to give clear zones of lysis at the characteristic MW of uPA. This technique was performed as previously described in Roche *et al* (36). Briefly, 2% casein Hammarsten was added to 10% SDS-PAGE gels +/- 2 mg/ml of plasminogen. Cell homogenates were then loaded directly onto each gel. The samples were not boiled or reduced prior to loading in order to retain enzymatic activity. After electrophoresis, the gels incubated in 2.5% Triton X-100 in H_20 for 1 hr. The gels were then incubated in 0.1 M glycine-NaOH buffer pH 8.4 for 4-6 hours at 37°C. Following incubation, the gels were then stained with 0.025% Commassie blue R-250, 40% methanol, 7% acetic acid overnight. The gels were destained in 40% methanol and 7% acetic acid for 1-2 hours

Western Blot to visualize uPA and its receptor uPAR:

Lewis lung carcinoma cellular homogenates were subjected to electrophoresis on a 10% resolving/ 5% stacking polyacrylamide gel. Gels were then electrophoretically transferred onto PVDF membranes (incubate PVDF membrane in 100% methanol for 15 seconds and then place in ddH_20 until ready to electroblot). The membrane was blocked for 1 hour with 1% BSA in wash buffer (consisting of NaCl, 1M Tris-HCl pH 7.4, Tween 20, and ddH_20). Polyclonal rabbit anti-human uPAR (gift from Dr. Andrew Mazar, Ångstrom Pharmaceuticals, La Jolla, CA) was used at a 1:10000 dilution of 2 mg/ml to detect mouse uPAR. In addition, polyclonal rabbit anti-rodent uPA IgG (obtained from American Diagnostica Inc, Greenwich, CT) was used at a 1:1000 dilution of 5 μg/ml to detect mouse uPA. Membranes were incubated with respective primary antibodies overnite at 4°C. Membranes were washed extensively with wash buffer for 20 minutes. PVDF membranes incubated in secondary antibody (goat anti-rabbit peroxidase conjugates diluted at 1:50000 in wash buffer) for 1hour at room temperature. Once again, the membranes were washed as done previously after primary antibody incubation. The bands were detected using SuperSignal Substrate System (Pierce Chemical, Rockford, IL). The protein bands were visualized on Hyperfilm ECL (Amersham, Buckinghamshire, England).

RT-PCR (Reverse-Transcriptase-Polymerase Chain Reaction):

Total RNA was isolated from 3LL (Lewis lung carcinoma) cells using RNeasy columns (Qiagen, Valencia, CA). cDNA synthesis was performed using the RT-PCR kit from Stratagene (La Jolla, CA). The following primers were used:

Table 2.1

Primer	Forward primer (5′-3′)	Reverse primer (5′-3′)
Mouse uPA	TCCTTTAAATGTGGTGGGAG	GTGTAGACACCGGGCTTGTT
Mouse uPAR	AGGACCTCTGCAGGACTACC	TGAAAGGTCTGGTTGCTATG

PCR amplification was done using the HotStarTaq Polymerase protocol. The PCR master mix contained 10x PCR buffer (3 uL), 25 mM $MgCl_2$ (1.2 uL), dNTP mix (10 mM of each at 0.6 uL), forward primer (1 uL at 30 pmol/uL), reverse primers (1 uL at 30 pmol/uL), HotStarTaq DNA Polymerase (0.5 uL), and distilled water (21.9 uL). After sufficient mixing, the master mix is dispensed into appropriate volumes into PCR tubes. Template DNA is added to individual tubes and the thermal cycler is programmed around the melting points of primers used. The reaction was heat activated for 15 min. at 95°C, denatured for 30 seconds at 94°C, annealed for 30 seconds at 60°C, and finally extended for 45 seconds at 72°C for a total of 35 cycles. After RT-PCR, each PCR reaction is loaded onto a 1% agarose gel and run on an electorphoretic chamber. Ethidium bromide is added to the agarose gel to allow visualization of bands under UV light.

Cell Proliferation Assay:

The MTT (tetrazolium salt)-cell proliferation assay is a quantitative colorimetric assay for measurements of cellular proliferation, viability, and cytotoxicity (Holst-Hansen, 1998). A standard curve was prepared after SVEC cells are harvested and counted. The curve consisted of known cell concentrations taken from 1:2 serial dilutions, ranging

from $2x10^5$ cells/ml to 3125 cells/ml. The standard curve assay was incubated at different time points (without drug treatment) at 37°C in 5% CO_2. In addition to the standard curve assay, an MTT assay was prepared with harvested cells at a concentration of $5x10^4$ cells/ml. The cells were treated with different concentrations of doxorubicin (0.05 μM, 0.1 μM, 0.2 μM, 0.4 μM, 0.6 μM, 0.8 μM and 1.0 μM) to plot a dose-response curve. Drug-treated MTT assays were checked at 24 hour and 48 hour time periods. At designated time period, 100 μl of MTT solution from a 1:5 preparation of MTT in 1xPBS was added to each well. The assay plate was then incubated at 37°C for 3 hours and then centrifuged for 10 minutes at 3000 rpm. The media supernatant was carefully pipetted out without disturbing the cell pellet. DMSO (250 μl) was added to each well to disrupt the cell pellet, hence cell lysis. The samples (200 μl) were transferred to a 96-well ELISA plaste and read at 540 nm with an ELISA reader. A blue color appeared that increased with higher cell concentration.

Transfilter Matrigel Invasion Assay:

The ability of tumor cells to traverse basement membrane and degrade extracellular matrix components (Type IV collagen, laminin) was measured using Matrigel-coated invasion chambers (37). The apparatus contains two chambers (upper and lower) that are separated by a microporous polycarbonate filter, the upper surface of which is coated with a thin layer of Matrigel (a reconstituted basement membrane extract derived from the Engelbreth-Holm Swarm tumor. Tumor cells are placed on the upper chamber where they settle onto the Matrigel layer. In the lower chamber a chemotactic agent can be

placed to stimulate directional cell migration of cells that invade the Matrigel layer. Usually, the invasive cells are found on the lower surface of the filter. A preliminary experiment was done using HT1080 cells and a negative control (3T3 fibroblast cell line). HT1080 and 3T3 cells were cultured and harvested using EDTA to detach cells from the flask. After one wash with RPMI 1640 only medium, cells were resuspended in 0.1% BSA, RPMI 1640 at a final concentration of $1x10^5$ cells/ml. 0.75 ml of 3T3 conditioned medium as the chemoattractant for HT1080 and 3T3 cells was then added to the bottom chamber of the wells. A total of 0.5 ml of cell suspension was added to the top chamber, which contains 50000 cells/well. The plates were incubated for 24 hours at 37°C, 5% CO_2 atmosphere. To quantitate the number of cells in the bottom well which invaded through the Matrigel filter, EDTA was used to detach the cells (HT1080) and the cells were collected. Quantitative analysis of the recovered cells was performed using a hemocytometer. Cells on the inside of the top wells were removed by cotton swab. Cells attached to the underside of the filter were fixed with methanol, stained with Geimsa, and then counted using an ocular grid under light microscopy. Similarly, an invasion assay was performed using 3LL cells with or without treatment of the anti-angiogenic compound Å6. First, two flasks of 90% confluent 3LL cells were washed with RPMI 1640 only (serum-free) medium three times, and then incubated in (0.2% BSA RPMI 1640) with Å6 (100 μM) or without overnight at 37°C, 5% CO_2. The 8 μM filter pore on the transwells contains 30 μg/filter Matrigel and 500 ng/ filter plasminogen. The Matrigel was rehydrated with RPMI 1640 only medium. The 3LL cells were detached from their flask using EDTA. The cells were suspended in serum free medium at a final

concentration of $1x10^5$ cells/ml. 500 µl of cell suspension was added to the top of the well. Then, 750 µl of 3T3 conditioned medium (0.2% BSA RPMI 1640) was added to the bottom chamber of the well. Moreover, Å6 was added to the top and bottom chambers of test group wells. Finally, plasminogen was added at a 500 µM concentration to the top of all wells. The assay was incubated for 48 hours at 37°C with 5% CO_2. Cells were quantitated as done with HT1080 cells. The assay was performed twice and results were similar. A one-tailed T-distribution revealed statistically significant results.

Endothelial Cell Tube Formation Assay:

The bottom of each well in a 24-well tissue culture plate was coated with 200 µl of (7.0 mg/ml Matrigel). Matrigel was allowed to polymerize for 1 hour in a 37°C incubator. $1x10^5$ small vessel endothelial cells/ml of media were added to each well. Treatment is as follows: Control (no treatment), Å6 (100 µM), Å6 (10 µM), Å6 (1 µM), Doxorubicin (0.05 µM), Å6 (100 µM) + Doxorubicin (0.05 µM), and Å6 (10 µM) + Doxorubicin (0.05 µM). Tube formation was photographed with a digital camera and viewed under light microscopy.

In vivo mouse study (C57 black mice):

6 Sample group treatments (each treatment group comprised of 7 mice) were studies as enumerated in Table 2.2

Test Group No.	Treatment
1	No Treatment (control)
2	Doxorubicin (8 mg/kg/day)
3	Doxorubicin (15 mg/kg/day)
4	Å6 (75 mg/kg/day)
5	Å6 (75 mg/kg/day) + Doxorubicin (8 mg/kg/day)
6	Å6 (75 mg/kg/day) + Doxorubicin (15 mg/kg/day)

Table 2.2 Test group summary

Tail vein injection of $1x10^5$ 3LL tumor cells per mouse was administered to each group on day one. The subsequent treatments received by the different groups are shown in Table 2.3.

	Treatment					
	Group 1	Group 2	Group 3	Group 4	Group 5	Group 6
Day 1	Dulbecco's PBS (.2ml per mouse) once a day i.p.			200 ul of Å6 (9.324 mg/ml) per mouse once a day i.p.		
Day2, 3 onto Day 21	200 ul of PBS per mouse twice a day i.p			200 ul of Å6 (4.662 mg/ml) per mouse twice a day i.p.		
Day 4	200ul of PBS per mouse once a day i.p	200 ul of doxorubicin (0.94 mg/ml) per mouse once a day i.p.	200 ul of doxorubicin (1.76 mg/ml) per mouse once a day i.p	200 ul of Å6 (4.662 mg/ml) per mouse once a day i.p.	200 ul of doxorubicin (0.94 mg/ml) per mouse once a day i.p.	200 ul of doxorubicin (1.76 mg/ml) per mouse once a day i.p.

Table 2.3 Treatment summary

Mice were sacrificed on day 21. We injected 1.0 ml of 33% Histo prep into the lungs, extracted the lungs from each test group, and then preserved them in Formalin solution. Tumors were counted under an optical microscope.

CHAPTER 3

RESULTS

1. Expression of uPA and uPAR in Lewis lung carcinoma cells:

Urokinase plasminogen activator when bound to its cell-surface receptor (uPAR) initiates a cascade of events, which ultimately leads to basement membrane destruction, thus fueling tumor invasion and metastasis. In addition to tumor invasion and metastasis, the uPA system plays a role in tumor angiogenesis. The ligation of uPAR by uPA on endothelial cells stimulates several pathways leading to endothelial cell differentiation and capillary tube formation on Matrigel (5). Therefore, uPA and uPAR expression are potential therapeutic targets when investigating anti-metastatic properties of Å6, since Å6 partially inhibits the binding of uPA to its receptor uPAR.

The initial set of experiments utilized a reverse-transcriptase polymerase chain reaction (RT-PCR) to detect uPA and/or uPAR gene expression in Lewis lung carcinoma (3LL) cDNA. 3LL cellular DNA was amplified with mouse uPA, mouse uPAR, and control mouse glyceraldehyde-3-phosphate dehydrogenase (GAPDH) primers. The resulting products were examined on a 1% agarose gel containing ethidium bromide and visualized by UV

transillumination. Both uPA and uPAR genes were expressed at their respective base pair locations of 614 and 430 respectively (Figure 3). Two repeat experiments showed similar results.

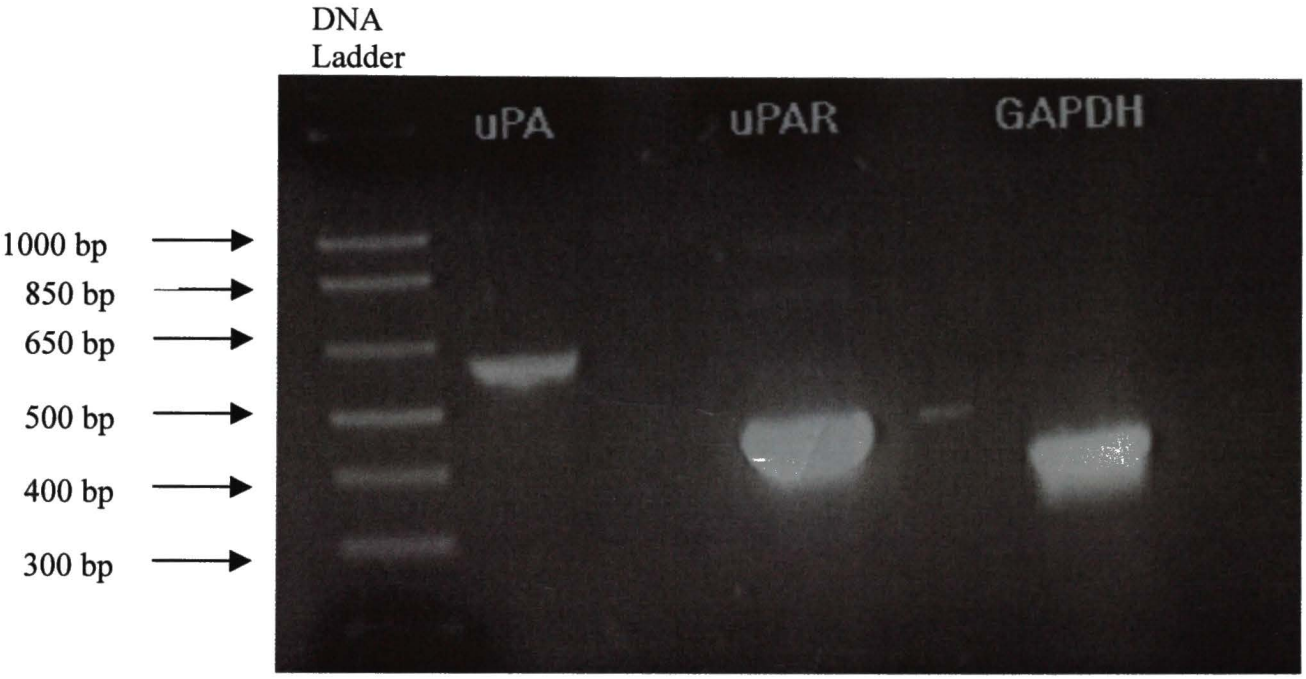

Figure 3. Reverse-Transcriptase-Polymerase Chain Reaction (RT-PCR) analysis of uPA and uPAR in Lewis Lung cDNA

Total RNA was isolated from Lewis Lung carcinoma (3LL) cells. RNA was converted to cDNA using RT-PCR kit from Stratagene (La Jolla, CA). 3LL cDNA was amplified with mouse uPA, mouse uPAR, and control mouse glyceraldehydes-3-phosphate dehydrogenase (GAPDH) primers. The PCR reaction was loaded onto a 1% agarose gel and run on an electrophoretic chamber. Bands were visualized under UV light.

Next, I wanted to show uPA and uPAR expression on the protein level. I prepared 3LL homogenates (described in Methods) and estimated protein concentration by using a Bicinchoninic Acid Protein Assay Kit (Sigma). The cell homogenate contained 53.8 μg of protein per 15 μl of sample. The sample was run on an SDS-PAGE gel and

electroblotted on a PVDF membrane. Urokinase plasminogen activator was visualized at a M_r of 50,000 daltons (Figure 4).

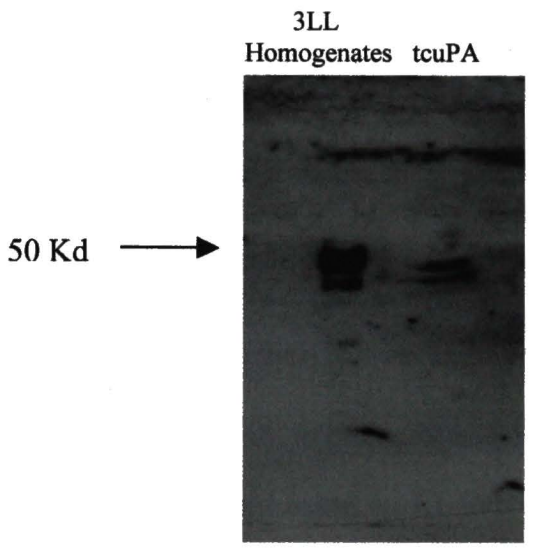

Figure 4a. Western Blot Analysis of uPA in 3LL homogenates
Cell homogenates were prepared as described in "Methods." The homogenates were then subjected to electorphoresis and transferred to a PVDF membrane. The membrane was treated with anti-uPA antibodies and the bands were detected using SuperSignal Substrate System (Pierce Chemical, Rockford, IL). The protein bands were visualized on Hyperfilm ECL (Amersham, Buckinghamshire, England).

In addition, human two-chain urokinase plasminogen activator was run as a positive control with a M_r of 50,000 daltons. Apparent molecular weights were calculated by generating a standard curve (by plotting the log of molecular weight on the y-axis vs the distance migrated on the x-axis). Then, the distance migrated was plugged back into the equation for the best-fit line to generate the calculated molecular weights (Figure 4b).

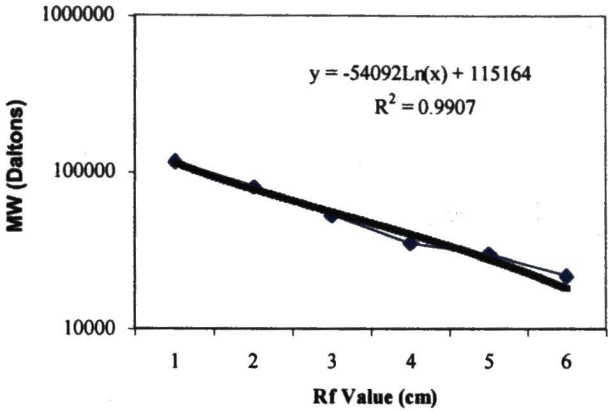

Figure 4b. Rf Value Plot of uPA in 3LL homogenates

The apparent molecular weight of uPA in 3LL homogenates was calculated by generating a standard curve (plot the log of molecular weight on the y-axis vs. the distance migrated on the x-axis). The distance migrated was plugged back into the equation for the best-fit line to generate the molecular weight of uPA.

Similarly, urokinase plasminogen activator receptor was expressed in 3LL homogenates at bands of 55,000 daltons, 34,000 daltons, and 30,000 daltons (Figure 5). Apparent molecular weights were calculated using an Rf Value Plot (Figure 5b). Soluble uPAR (suPAR) from Drosophila was loaded as a positive control and was given to us from collaborators in San Diego. A band was visualized at 35,000 daltons.

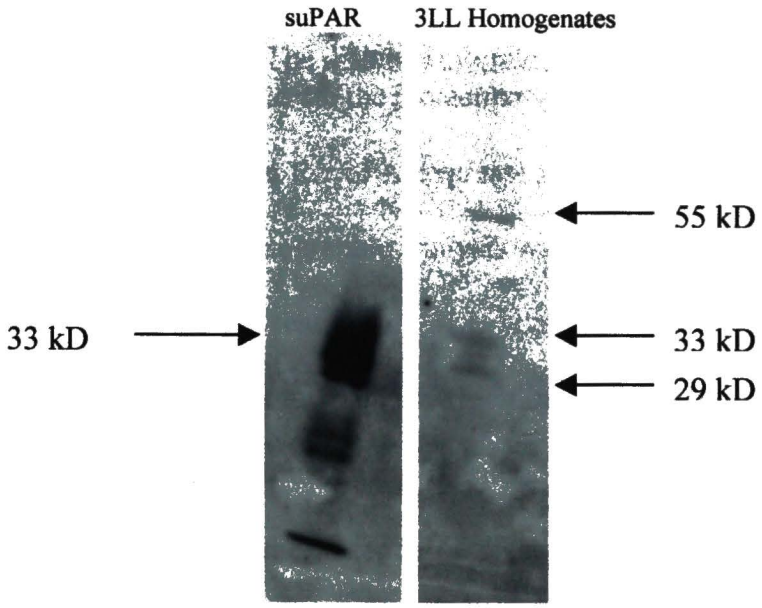

Figure 5a. Western Blot Analysis of uPAR in 3LL homogenates
Cell homogenates were prepared as described in "Methods." The homogenates were electrophoresed and transferred to a PVDF membrane. The membrane was then treated with anti-uPAR antibodies and the bands were detected and visualized on Hyperfilm ECL.

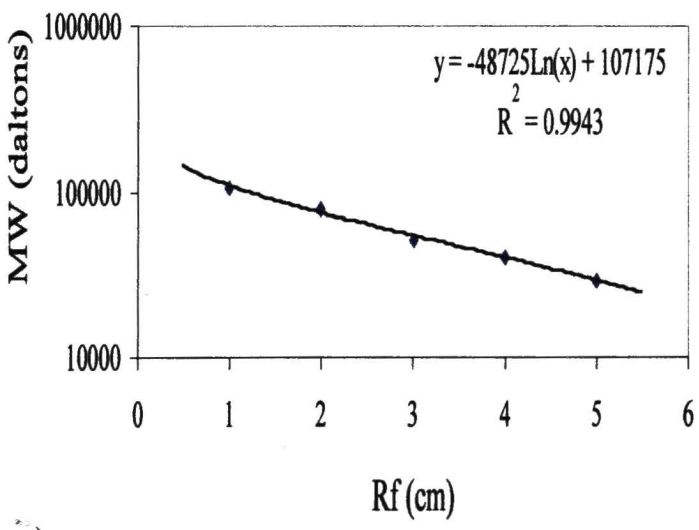

Figure 5b. Rf Value Plot of uPAR in 3LL homogenates

The apparent molecular weight of uPAR in 3LL homogenates was calculated by generating a standard curve (plot the log of molecular weight on the y-axis vs. the distance migrated on the x-axis). The distance migrated was plugged back into the equation for the best-fit line to generate the molecular weight of uPAR.

Moreover, I wanted to make sure the uPA expressed on my Western blot was indeed active uPA. For this purpose, zymographic analysis was used to observe enzyme activity (procedure in Methods). Before testing my 3LL homogenates, I did a few trials with human fibrosarcoma (HT1080) homogenates which have been shown to express active uPA. The zymography confirmed urokinase plasminogen activator expression, because its plasminogen dependent. In the absence of plasminogen, zones of lysis were not detected. Two-chain uPA was loaded as a positive control alongside the homogenates, similar to the western blot done previously. After Coommassie staining, a zone of lysis was detected at a M_r of 49,000 daltons in the 3LL homogenates. Another high molecular weight form of uPA was was visualized at a M_r of 77,000 daltons. Human two-chain uPA was detected at 57,000 daltons (Figure 6). Apparent molecular weights were calculated using an Rf Value Plot (Figure 6b). Zymographic analysis was repeated 3 times, giving similar results each time.

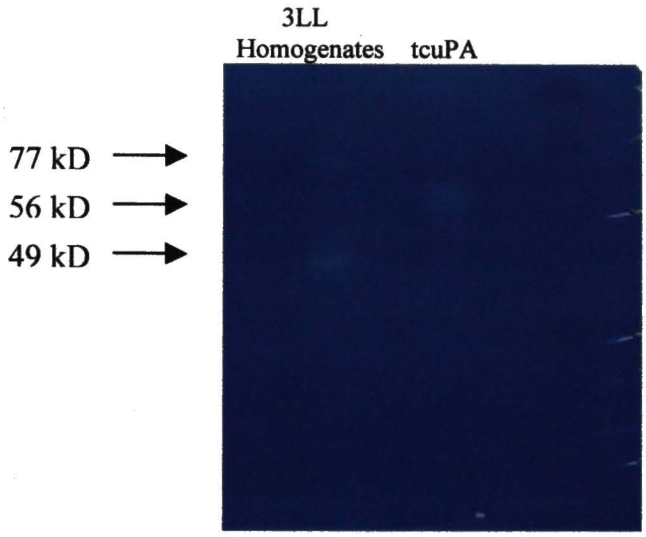

Figure 6a. Zymographic Analysis of uPA in 3LL homogenates

Cell homogenates were prepared as described in "Methods." Casein was added to 10% SDS-PAGE gels +/- plasminogen. Cell homogenates were loaded directly onto each gel. The gels incubated in 2.5% Triton X-100 in H_2O for 1 hour. The gels were then incubated in 0.1 M glycine-NaOH buffer pH 8.4 for 4-6 hours. Following incubation, the gels were stained with 0.025% Commassie blue R-250, 40% methanol, and 7% acetic acid overnight. The gels were destained in 40% methanol and 7% acetic acid for 1-2 hours. This experiment was performed three times giving similar results.

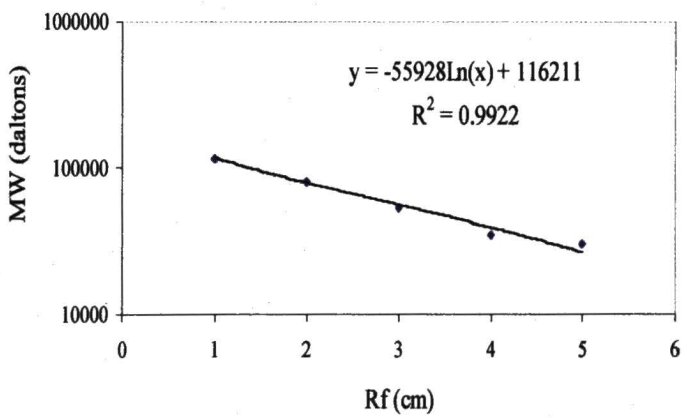

Figure 6b. Rf Value Plot of uPA in Zymographic Analysis

The apparent molecular weight of uPA in 3LL homogenates was calculated by generating a standard curve (plot the log of molecular weight on the y-axis vs. the distance migrated on the x-axis). The distance migrated was plugged back into the equation for the best-fit line to generate the molecular weight of uPA.

2. Investigate invasiveness of 3LL carcinomas +/- Å6 in an *in vitro* Matrigel invasion assay:

The invasion assay was performed as explained in (Methods). Preliminary experiments tested the invasiveness of human fibrosarcoma (HT1080) cells through a reconstituted matrix (Matrigel). Results indicated HT1080 was significantly more invasive compared to my negative control 3T3 cells. A one-tailed t-distribution revealed significance, p=0.005 (figure 7).

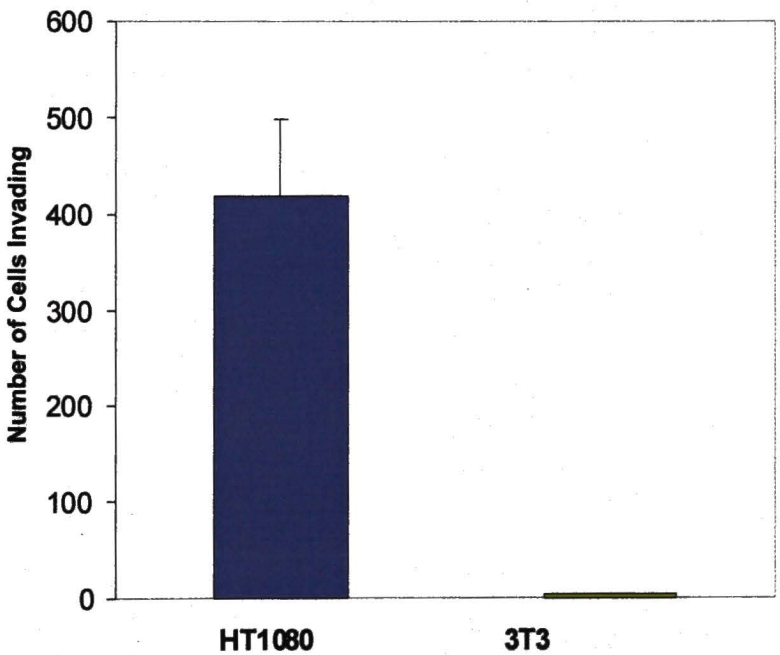

Figure 7. Invasion Assay with HT1080 (fibrosarcoma cells)

HT1080 (fibrosarcoma cells) and 3T3 (fibroblast cell line used as a negative control) were cultured and harvested. The cells were resuspended in 0.1% BSA, RPMI 1640 at a final concentration of $1x10^5$ cells/ml. The plates were incubated for 24 hours. Cells in the bottom well

were quantitated using a hemocytometer. Cells attached to the underside of the filter were stained with Geimsa and counted.

Next, the more invasive aggressive Lewis lung carcinoma cells were pretreated with or without Å6. Tumor cells, which passed through the 8 μM filter pore, were counted. The invasion index was determined using the following formulas:

% invasion= (Mean number of cells which invaded/mean number of cells which migrated through noncoated transwell) X100

Invasion index= % invasion of experimental cells/% invasion of control cells.

All determinations were performed in triplicate. Å6 inhibited the invasion of Lewis lung carcinoma cells by 40-45% compared to control (w/o Å6) (Figure 8). A one-tailed t-distribution revealed significance, p value=0.01.

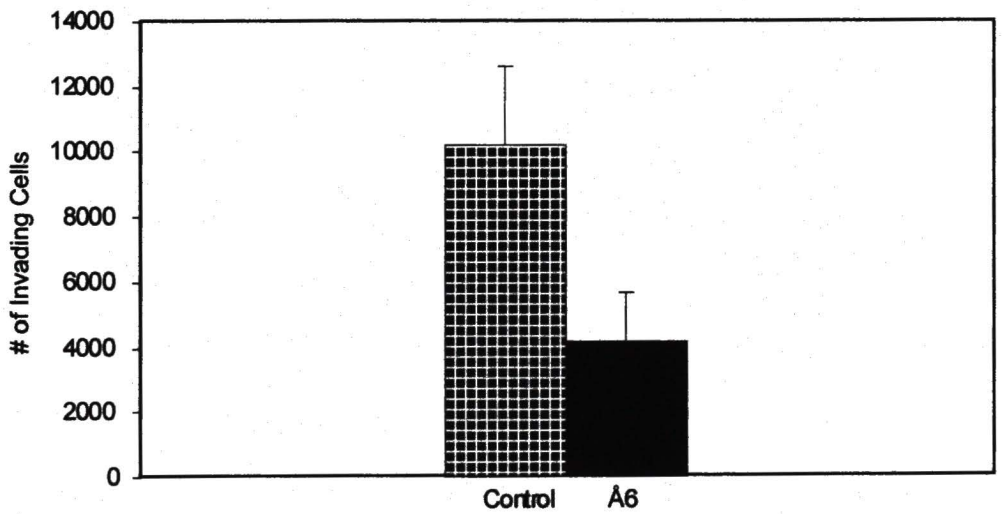

Figure 8. Invasion Assay with 3LL (+/- Å6)
The invasion assay was performed as described in "Methods." An MTT proliferation assay was used as a control to measure the proliferation of 3LL cells with and without Å6 to verify the non-toxicity of Å6. Å6 did not have any effect on cell proliferation, thus did not kill the cells in the

invasion assay (data not shown). This assay was performed twice with similar results. A one-tailed t-distribution revealed significance, p value=0.01

The MTT assay was used as a control to measure proliferation of 3LL cells with and without Å6 to verify non-toxicity of Å6. Å6 did not have any effects on the proliferation of the tumor cells, thus Å6 did not kill the cells in the invasion assay.

3. **Observe and quantitate anti-angiogenic properties of Å6 in an *in vitro* endothelial cell tube formation assay:**

Small vessel endothelial cells (SVEC) were plated on Matrigel (see Methods).

Endothelial cell tube formation assays suggest differences in thickness (width) of tubes after 8 hours of incubation on Matrigel coated wells (Figure 9).

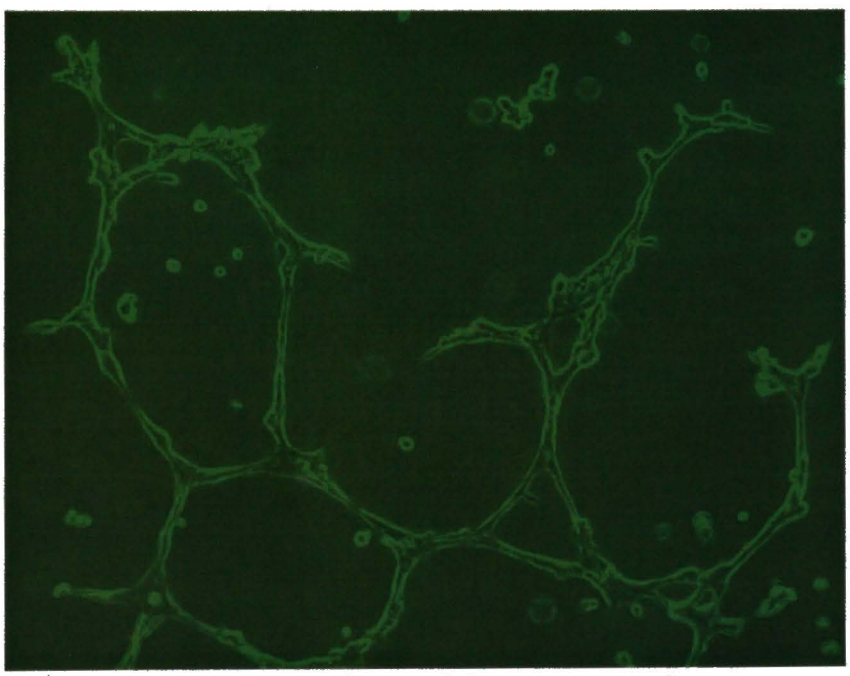

Figure 9a. Control (no treatment)

Small vessel endothelial cells (SVEC) extracted from mice were grown on Matrigel-coated wells without treatment.

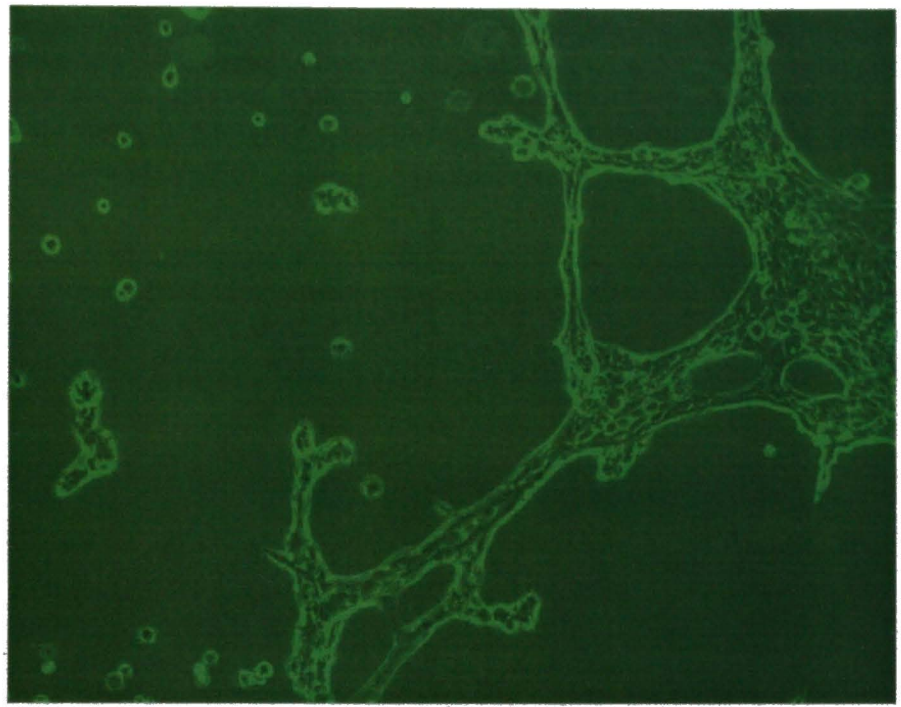

Figure 9b. Å6 (100 uM)

SVEC were grown under same conditions as control cells, however Å6 (100 uM) was added to the resuspended cells prior to incubation.

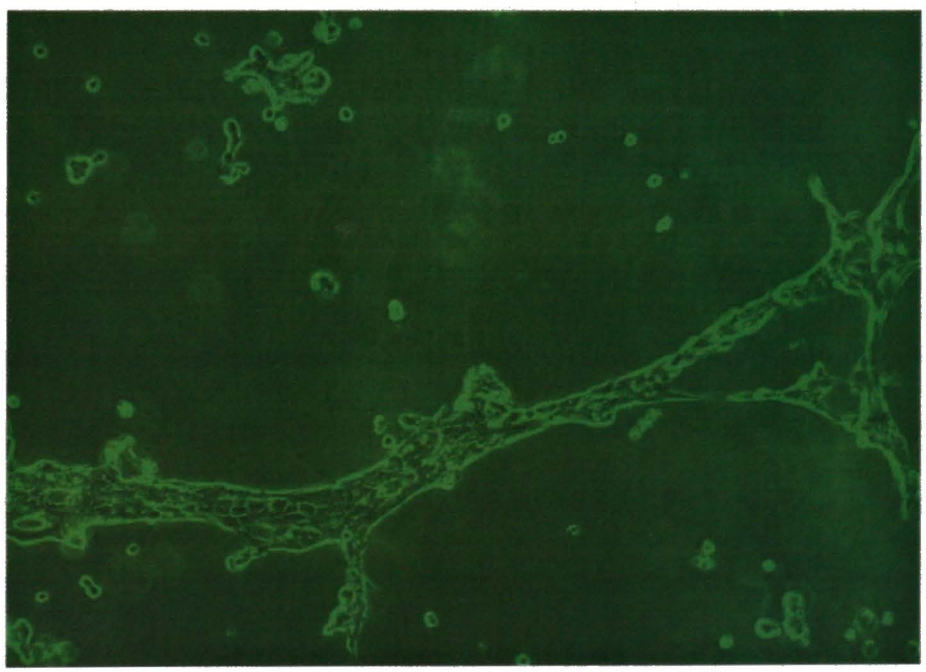

Figure 9c. Doxorubicin (0.05 uM)

SVEC were grown and harvested as done in control and Å6-treated wells. Doxorubicin (0.05 uM) was added to the resuspended cells prior to incubation. A MTT proliferation assay tested the cytotoxicity of doxorubicin on SVEC, described in the "Methods" section. 0.05 uM of doxorubicin did not kill the SVEC, and therefore this concentration was used in the tube formation assay (data not shown).

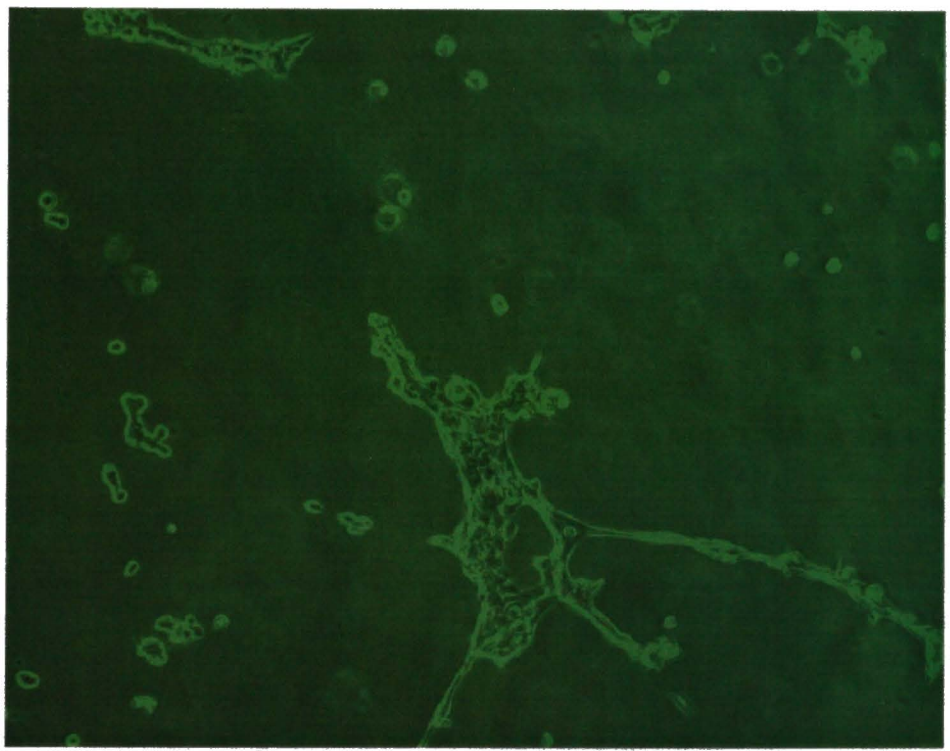

Figure 9d. Å6 (100 uM) and doxorubicin (0.05 uM)

A combination of Å6 and doxorubicin were added to the SVEC prior to incubation.

In the absence of Å6, approximately 75% of the total tube number exhibited slender (<60 uM) and more defined tube formations. However, when treated with 100 uM of Å6, 40% of the total tube population displayed tubes of <60 uM. Doxorubicin-treated wells resembled the Å6-treated wells with respective tube thickness. The combination treatment of Å6 (100 uM) and doxorubicin (0.05 uM) on SVEC tube formation showed a slightly higher percentage (70%) falling under the >60 uM, compared to either Å6 alone

(61%) or doxorubicin alone (63%). However, neither synergy nor additivity was detected in the combination groups. Å6-treated wells at 10 uM and 1 uM did not show morphological change with respect to thickness compared to control (non-treated) wells. One-tail t-distributions with unequal variances for control vs Å6, control vs. doxorubicin, and control vs. Å6+doxorubicin show p-values at 0.009, 0.0005, 0.0002 respectively (Figure 10).

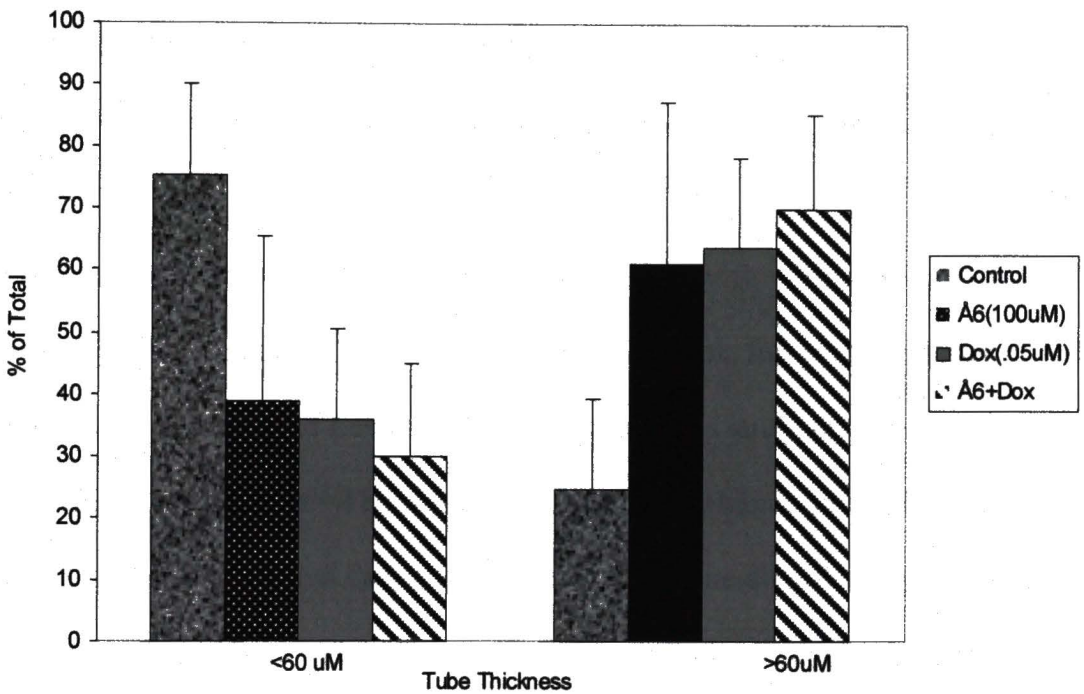

Figure 10. Degrees of tube thickness between the test groups in the endothelial cell formation assay.
Tube thickness was measured with a digital camera and viewed under light microscopy. This experiment was conducted with repeatable results. Significance was measured using a one-tailed t-distributions with unequal variances for control vs. Å6, control vs. doxorubicin, and control vs. Å6 + doxorubicin. P-values are 0.009, 0.0005, 0.0002 respectively.

4. Does combination treatment using Doxorubicin and Å6 have a synergistic effect on reducing experimental cancer metastases in an *in vivo* Lewis lung carcinoma mouse model compared to either agent alone?

Dr. Goldfarb in collaboration with Dr. Rabbani and others have shown that Å6 exhibits anti-tumor activity against several tumor types when administered alone and shows enhanced therapy when combined with a cytoreductive chemotherapeutic agent *in vivo* vs. either agent alone (29). For instance, cyclophosphamide in combination with Å6 had an additive effect on Lewis lung carcinomas compared to either agent alone (2). In addition, Å6 or cisplatin alone suppressed subcutaneous tumor growth *in vivo* by 48% and 53% respectively, and the combination of Å6 and cisplatin inhibited glioblastoma growth by 92% (28).

Therefore, I have extended this work with doxorubicin (standard chemotherapeutic agent) in combination with Å6 to look for possible synergy and/or additivity in the treatment of Lewis lung carcinomas. This study involved six test groups with 7 (C57/Bl) mice each. The dosing regiment is explained in the Methods section (Table 2.1, 2.2). The *in vivo* data indicated that Å6 alone significantly reduced tumor burden by at least 50% (Figure 11). The doxorubicin treatment (15 mg/kg/day) effectively eradicated tumors, unfortunately its well known toxicity caused the expiration of 2 out of 7 mice. The combination groups of doxorubicin and Å6 showed similar therapeutic effects to both the doxorubicin alone and Å6 alone test groups. Neither synergy nor additivity was detected using combination therapy. Experimental significance was determined using ANOVA statistical analysis, $p=0.0001$ (Figure 11).

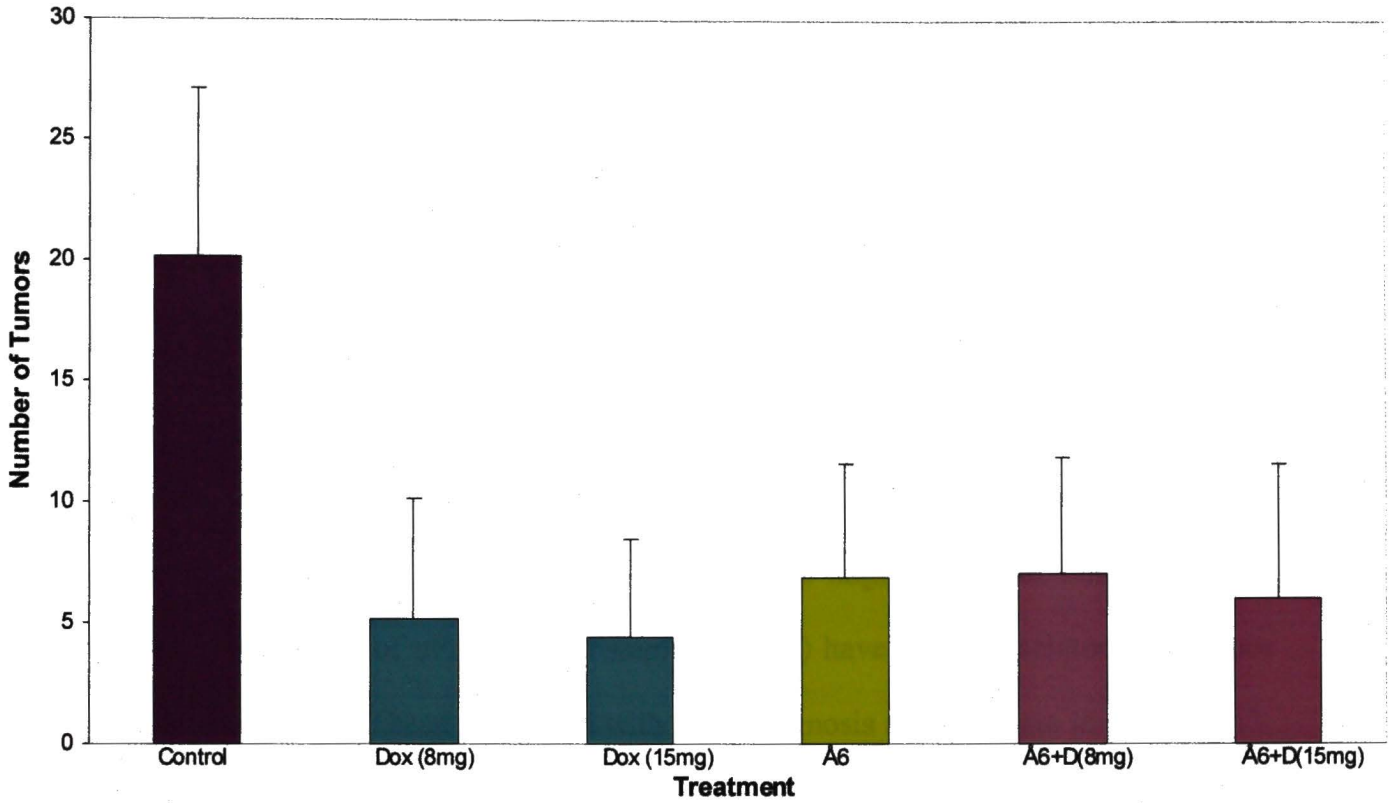

Figure 11. Treatment of Å6 and/or doxorubicin on 3LL carcinomas.

The *in vivo* Lewis Lung carcinoma mouse model was performed as described in "Methods." Experimental significance was determined using ANOVA statistical analysis, p=0.0001.

CHAPTER 4

DISCUSSION

The urokinase plasminogen activator (uPA) system has a plethora of functions including the progression, invasion, metastasis, and angiogenesis of numerous solid tumors. Expression of uPA and its receptor (uPAR) have been associated with tumor progression and have been correlated with poor prognosis and outcome in patients (13, 29). In addition, several intracellular pathways are initiated when uPA binds to uPAR including activation of the MAP kinase pathway, chemotaxis regulation, the up-regulation of oncogene expression, and stimulation of cell adhesion (29). Moreover, receptor binding results in the activation of the zymogen form of uPA (scuPA) into active two-chain uPA. This leads to downstream activation of plasminogen and matrix metalloproteinases, which ultimately contribute to basement membrane degradation. This proteolytic flux in combination with uPA-dependent intracellular signaling results in acceleration of tumor cell invasion and tumor-associated angiogenesis (29).

Urokinase plasminogen activator interacts with its receptor via its growth factor domain (aa 1-48 of uPA). Nevertheless, a second site has been identified in uPA that interacts with uPAR. This connecting peptide composed of aa 136-143 of uPA is termed Å6. Å6 partially inhibits the binding of uPA to uPAR in a noncompetitive manner. Therefore, it was imperative to document that the Lewis lung carcinoma cell line

expresses both uPA and its receptor uPAR in order to test the potential therapeutic effects of Å6 in this model system. RT-PCR confirmed the uPA and uPAR genes are expressed in 3LL cDNA, confirming and extending previous findings (32,33). Western blot analysis identified protein expression of both uPA and its receptor at their respective molecular weights in good agreement with the literature. Murine uPA was detected at a molecular weight of 50, 582 daltons. Urokinase plasminogen activator receptor was visualized at a characteristic M_r of 55,296 daltons. In addition, lower molecular forms of uPAR were detected at Mr of 33,888 daltons and 29,735 daltons. The 33,888 and 29,735 dalton bands can be described as two alternatively spliced mouse urokinase receptor mRNAs (7). In addition, zymographic analysis verified that the uPA observed in the western was indeed active two-chain uPA. Zones of lysis were detected at Mr of 49 kD and 77 kD. The 49 kD band has been well documented in Lewis lung carcinoma cells (33). The 77 kD band may correspond to tissue-type plasminogen activator (t-PA) which plays a role in plasminogen activation leading to thrombolysis (32). On the other hand, the 77 kD band may indicate a higher molecular weight form of uPA, since uPA is known to exist in both low and high molecular weight forms (33).

After molecular and immunological analysis of uPA and uPAR gene and protein expression, I then wanted to elucidate the effects of Å6 on Lewis lung tumor cells *in vitro*. Generally, three mechanisms have been invoked to explain tumor cell invasion: the rapid multiplication of malignant cells leading to growth and infiltration by mechanical pressure; destruction of the host tissue via proteolytic enzymes produced by the tumor cell; and finally the lack of tumor cell adhesiveness is accompanied by an

increase in cell motility (2). I focused on the second mechanism of tumor invasion to test the effects of Å6 (100 μM) of tumor invasiveness through a simulated basement membrane (Matrigel). Å6 exhibited a direct effect on tumor invasiveness by inhibiting the invasion of Lewis lung carcinoma cells through the simulated basement membrane (Matrigel) by approximately 45%. This finding is consistent with data showing anti-invasive effects of Å6 in a human breast adenocarcinoma cell line (MDA-MB-231), and rat mammary adenocarcinoma cell line (Mat B-III) (29). Several proteolytic pathways are involved in the destruction of ECM (i.e. Matrix Metalloproteinases) which explains why Å6 inhibits tumor invasion by 45%, rather than 100%.

Next, I asked whether anti-angiogenic properties are noted of Å6 on endothelial cell tube formation. The endothelial cell tube formation assay is a well-documented assay (18, 19, 20, 21) that allows for aspects of angiogenesis to be studied *in vitro*. In appropriate conditions, capillary endothelial cells when grown on Matrigel will form tubular networks that are almost identical, by light and electron microscopy, to capillary vascular beds *in vivo* (18). Our laboratory and collaborators have shown a disruption of lung filaments in human umbilical vein endothelial cells (HUVEC) when treated with Å6. I used a physiological cell line, the small vessel endothelial cells (SVEC) derived from mice. For the first time, I made a new and novel observation that there is a morphological change on tube formation when SVEC were treated with Å6, doxorubicin, or a combined treatment of Å6 and doxorubicin. When small vessel endothelial cells are treated with Å6, the tube formations appear thicker and shorter. This observation was supported using an Imaging software program that quantitated tube length and width.

Suprisingly, doxorubicin at (0.05 μM) also had an effect on tube morphology, giving rise to thicker tubes (>60 μM). Plum *et al* cited doxorubicin's (Adriamycin) effect on the inhibition of endothelial cell cord formation in a dose-dependent manner (35). The combination of doxorubicin and Å6 did not produce additive or synergistic effects in the small vessel endothelial cell tube network. However, Plum *et al* reported synergistic inhibition of endothelial cell tube formation using combinations of suboptimal doses of Adriamycin (doxorubicin) and rh-endostatin. This suggests the therapeutic potential of using suboptimal doses of Å6 and doxorubicin in the endothelial cell tube formation assay to assess synergy. We speculate that the thickening of tubes seen with Å6 implies anti-angiogenic properties, similar to what has been observed *in vivo* (29). Thicker tubes could potentially impede blood flow, thereby reducing available nutrients needed for tumors to grow. Moreover, endothelial cell images revealed partially disconnected tubes in the treatment groups, suggesting collapsed blood vessel formation. This work will be repeated using human lung microvascular endothelial cells (HMVEC) with suboptimal doses of both Å6 and doxorubicin.

The *in vivo* Lewis lung carcinoma mouse model was performed to test possible synergistic effects of Å6 in combination with doxorubicin. A low tumor burden (100,000 cells injected into the mouse tail vein) was used to count the number of lung metastases. Å6 alone (75 mg/kg/day) had an unexpected therapeutic effect on Lewis lung carcinoma metastases. This is the first observation that Å6 has the potential to display a direct anti-metastatic therapeutic effect for established pulmonary metastases in this model. Co-administration of Å6 (75 mg/kg/day) and doxorubicin (8 mg/kg/day) had an effect similar

to Å6 alone. When Å6 (75 mg/kg/day) doses were combined with doxorubicin at a higher concentration (15 mg/kg/day), the toxicity of doxorubicin caused morbidity in the test group mice. This experiment was repeated with a higher tumor burden of $1.5x10^5$, however Å6 did not have a direct effect on successfully treating Lewis lung metastases. Doxorubicin at high doses could have masked the effect of Å6, giving rise to toxic side effects. Therefore, lower amounts of doxorubicin (i.e. 4 mg/kg/day) combined with Å6 (75 mg/kg/day) may have the desired synergistic effect, with reduced risk of harmful toxicities. Additional studies beyond the scope of this thesis will be required to fully evaluate this effect.

In addition, tumor cells readily acquire resistance to cytotoxic chemotherapy, which is not expected for vascular endothelial cells. Folkman *et al* proposed an alternative dosing schedule (anti-angiogenic scheduling of chemotherapy) to effectively treat experimental drug-resistant cancer (such as Lewis lung carcinoma). To more effectively suppress endothelial cell proliferation within the tumor, a dosing schedule was developed that administered the chemotherapeutic agent at shorter intervals without interruption (28). Similarly, doxorubicin (chemotherapeutic agent) administered at a suboptimal dose combined with regular doses of Å6 (75 mg/kg/day) extended over a longer time course (~100 days) allow for better long-term survival. This treatment minimizes drug-resistance in tumor populations as well as diminishing toxic side effects (seen in most chemotherapeutic regimens).

In sum, this thesis revealed the potential of the angiogenic inhibitor (Å6) combined with chemotherapeutic agents (doxorubicin) to effectively treat cancer metastases. The

anti-invasive properties of Å6 coupled with its abililty to phenotypically change endothelial cell tube networks (*in vitro*) and reduce tumor burden (*in vivo*) make it an effective agent in Lewis lung carcinomas. I hypothesize synergy and/or additivity may be detectable as a result of these types of studies and serve as a model system for investigating other combination treatments. Additional studies are needed and must be designed to more broadly test this hypothesis in future studies.

REFERENCES

1. Goldfarb, R.H., Liotta, L.A.: Proteolytic Enzymes in Cancer Invasion and Metastasis. Seminars in Thrombosis and Hemostasis. 12(4):294-305, 1986.

2. Fidler,I.J., Gersten, DM, Hart, I.R.: The biology of cancer invasion and metastasis. Advanced Cancer Research. 28:150-165, 1978.

3. Heppner, G.H.: Tumor Heterogeneity. Cancer Research. 44:2259-2265, 1984.

4. Goldfarb, R.H., Brunson, K.W.: Ch. 1 Overview of Current Understanding of Tumor Spread in Cancer Growth and Progression. Edit. R.H. Goldfarb. Kluwer Academic Publishers: Dordrecht, Netherlands. Fundamental Aspects of Cancer. 28-32, 1989.

5. Mazar, A.P., Gawlak, S., Goldfarb, R.H., Kitson, R.P., Rabbani, S.A., Guo, Y., Gown, A.M., Jones, T.R.: The urokinase plasminogen activator receptor (uPAR) is a chokepoint for carcinoma metastasis and angiogenesis. Recent Res. Devel. Cancer. 2:1-12, 2000.

6. Mazar, A.P., Henkin, J., Goldfarb, R.H.: The urokinase plasminogen activator system in cancer: Implications for tumor angiogenesis and metastasis. Angiogenesis. 3:15-32, 1999.

7. Kristensen, P., Eriksen, J., Blasi, F., Dano, K.: Two Alternatively Spliced Mouse Urokinase Receptor mRNAs with Different Histological Localization in the Gastrointestinal Tract. The Journal of Cell Biology. 115(6):1763-1771, 1991.

8. Mazzieri, R., Masiero, L., Zanetta, L, Monea, S., Onisto, M., Garbisa, S., Mignatti, P.: Control of type IV collagenase activity by components of the urokinase-plasmin system: a regulatory mechanism with cell bound reactants. EMBO J. 16:2319-32, 1997.

9. Liotta, L.A., Goldfarb, R.H., Brundage, R., Siegal, G.P., Terranova, V., Garbisa, S.: Effect of plasminogen activator (urokinase), plasmin, and thrombin on glycoprotein and collagenous components of basement membrane. Cancer Research. 41:4629-4636, 1981.

10. Mulligan-Kehoe, M.J., Wagner, R., Wieland, C., Powell, R.: A truncated Plasminogen Activator Inhibitor-1 Protein Induces and Inhibits Angiostatin (Kringles 1-3), a Plasminogen Cleavage Product. The Journal of Biological Chemistry. 276(11):8588-8596, 2001.

11. Al-Atrash, G., Kitson, R.P., Xue, Y., Goldfarb, R.H.: Cooperation of Urokinase Plasminogen Activator and Matrix Metalloproteinases in NK Cell Invasion. In Vivo. 14, 2000.

12. Stahl, A., Mueller, B.M.: Binding of urokinase to its receptor promotes migration and invasion of human melanoma cells in vitro. Cancer Research. 54:3066-3071, 1994.

13. Stephens, R.W., Nielsen, H.J., Christensen, I.J., Thorlacius-Ussing, O., Sorensen, S., Dano, K., Brunnen, N.: Plasma urokinase receptor levels in patients with colorectal cancer: relationship to prognosis. Journal of the National Cancer Institute. 91(10):869-873, 1999.

14. Goldfarb, R.H., Ziche, M., Murano, G., Liotta, L.: Plasminogen Activators (Urokinase) Mediate Neovascularization: Possible Role in Tumor Angiogenesis. Seminars in Thrombosis and Hemostasis. 12(4):337-338, 1986.

15. Brower, V.: Tumor angiogenesis—new drugs on the block. Nature Biotechnology. 17:964-968, 1999.

16. Hanahan, D., Folkman, J.: Patterns and Emerging Mechanisms of the Angiogenic Switch during Tumorigenesis. Cell. 86:353-364, 1996.

17. Folkman, J.: How is Blood Vessel Growth Regulated in Normal and Neoplastic Tissue?—G.H.A. Clowes Memorial Award Lecture. Cancer Research. 46:467-473, 1986.

18. Folkman, J., Haudenschild, C.: Angiogenesis *in vitro*. Nature. 288:551-556, 1980.

19. Gamble, J.R., Matthias, L.J., Meyer, G., Kaur, P., Russ, G., Faull, R., Berndt, M.C., Vadas, M.A.: Regulation of In Vitro Capillary Tube Formation by Anti-Integrin Antibodies. The Journal of Cell Biology. 121(4):931-943, 1993.

20. Haralabopoulos, G.C., Grant, D.S., Kleinman, H.K., Lelkes, P.I., Papaioannou, S.P., Maragoudakis, M.E.: Inhibitors of Basement Membrane Collagen Synthesis

Prevent Endothelial Cell Alignment in Matrigel *In vitro* and Angiogenesis *In vivo*. Laboratory Investigation. 71(4):575-582, 1999.

21. Grant, D.S., Tashiro, K., Segui-Real, B., Yamada, Y., Martin, G., Kleinman, H.Y.: Two Different Laminin Domains Mediate the Differentiation of Human Endothelial Cells into Capillary-like Structures In Vitro. Cell. 53:933-943, 1989.

22. Strasly, M., Cavallo, F., Geuna, M., Mitola, S., Colombo, M.P., Forni, G., Bussolino, F.: IL-12 Inhibition of Endothelial Cell Functions and Angiogenesis Depends on Lymphocyte-Endothelial Cell Cross-Talk. The Journal of Immunology. 3890-3899, 2001.

23. Thompson, W.D., Li, W.W., Maragoudakis, M.: The clinical manipulation of angiogenesis: pathology, side-effects, surprises, and opportunities with novel human therapies. Journal of Pathology. 190:330-337, 2000.

24. O'Reilly, M.S., Homgren, L., Shing, Y., Chen, C., Rosenthal, R.A., Moses, M., Lane, W.S., Cao, Y., Sage, E.H., Folkman, J.: Angiostatin: A Novel Angiogenesis Inhibitor That Mediates the Suppression of Metastases by a Lewis Lung Carcinoma. Cell. 79:315-328, 1994.

25. Sim, B.K.L., O'Reilly, M.S., Liang, H., Fortier, A.H., He, W., Madsen, J.W., Lapcevich, R., Nacy, C.A.: A Recombinant Human Angiostatin Protein Inhibits Experimental Primary and Metastatic Cancer. Cancer Research. 57:1329-1334, 1997.

26. Kamphaus, G.D., Colorado, P.C., Panka, D.J., Hopfer, H., Ramchandran, R., Torre, A., Maeshima, Y., Mier, J.W., Sukhatme, V.P., Kalluri, R.: Canstatin, a Novel Matrix-derived Inhibitor of Angiogenesis and Tumor Growth. Journal of Biological Chemistry. 255(2):1209-1215, 2000.

27. Min, H.Y., Doyle, L.V., Vitt, C.R., Zandonella, C.L., Stratton-Thomas, J.R., Shuman, M.A., Rosenberg, S.: Urokinase Receptor Antagonists Inhibit Angiogenesis and Primary Tumor Growth in Syngeneic Mice. Cancer Research. 56:2428-2433, 1996.

28. Browder, T., Butterfield, C.E., Kraling, B.M., Shi, B., Marshall, B., O'Reilly, M.S., Folkman, J.: Antiangiogenic Scheduling of Chemotherapy Improves Efficacy against Experimental Drug-resistant Cancer. Cancer Research. 60:1878-1886, 2000.

29. Guo, Y., Higazi, A-R., Arakelian, A., Sachais, B.S., Gines, D., Goldfarb, R.H., Jones, T.R., Kwaan, H., Mazar, A.P., Rabbani, S.A.: A peptide derived from the non-receptor region of urokinase plasminogen activator (uPA) inhibits tumor progression and angiogenesis and induces tumor cell death *in vivo*. The FASEB Journal. 14:1-11, 2000.

30. Mishima, K., Mazar, A.P., Gown, A., Skelly, M. Ji, X., Wang, X., Jones, T.R., Cavenee, W.K., Su-Huang, H.J.: A peptide derived from the non-receptor binding region of urokinase plasminogen activator inhibits glioblastoma growth and angiogenesis *in vivo* in combination with cisplatin. PNAS. 97(15):8484-8489, 2000.

31. Shalinsky, D.R., Brekken, J., Zou, H., Bloom, L.A., McDermott, C.D., Zook, S., Varki, N.M., Appelt, K.: Marked Antiangiogenic and Antitumor Efficacy of AG3340 in Chemoresistant Human Non-Small Cell Lung Cancer Tumors: Single Agent and Combination Chemotherapy Studies. Clinical Cancer Research. 5:1905-1917, 1999.

32. Skriver, L., Larsson, L., Kielberg, V., Nielsen, L.S., Andresen, P.B., Kristensen, P., Dano, K.: Immunocytochemical Localization of Urokinase-type Plasminogen Activator in Lewis Lung Carcinoma. Journal of Cell Biology. 99:753-758, 1984.

33. Goldfarb, R.H.: Plasminogen Activators. Ann. Rep. in Medicinal Chem. 18:257-264, 1983

34. Larsson, L.I., Skriver, L., Nielsen, L.S., Grondahl-Hansen, J., Kristensen, P., Dano, K.: Distribution of urokinase-plasminogen activator immunoreactivity in the mouse. Journal of Cell Biology. 98:894-903, 1984.

35. Plum, S.M., Hanson, A., Volker, K.M., Sim, B.K.L., Fogler, W.E., Fortier, A.H.: Synergistic Effects of Recombinant Human Endostatin in Combination with Adriamycin on *in Vitro* Endothelial Cell Activity as Well as Tumor Growth *in Vivo*. Proc. Am. Assoc. Can. Rsh. 42:580, Abstract #3111, 2001

36. Roche, P.C., Campeau, J.D., Shaw, S.T., Jr.: Comparitive electrophoretic analysis of human and porcine plasminogen activators in SDS-polyacrylamide gels containing plasminogen and casein. Biochem Biophys Acta. 745:82-89, 1983.

37. Wakabayachi, H., Nicolson, G.L.: Transfilter Cell Invasion Assays. Cell Biology, A Laboratory Handbook: 2nd edition. 1:296-301, 1998.